An Improved Perturb and Observed Maximum Power Point Tracking Algorithm for Photovoltaic Power Systems

Rasool Kahani, Mohsin Jamil, and M. Tariq Iqbal

***Abstract*—This paper aims to improve the performance of the conventional perturb and observe (P&O) maximum power point tracking (MPPT) algorithm. As the oscillation around the maximum power point (MPP) is the main disadvantage of this technique, we introduce a modified P&O algorithm to conquer this handicap. The new algorithm recognizes approaching the peak of the photovoltaic (PV) array power curve and prevents the oscillation around the MPP. The key to achieve this goal is testing the change of output power in each cycle and comparing it with the change in array terminal power of the previous cycle. If a decrease in array terminal power is observed after an increase in the previous cycle or in the opposite direction, an increase in array terminal power is observed after a decrease in the previous cycle; it means we are at the peak of the power curve, so the duty cycle of the boost converter should remain the same as the previous cycle. Besides, an optimized duty cycle is introduced, which is adjusted based on the operating point of PV array. Furthermore, a DC-DC boost converter powered by a PV array simulator is used to test the proposed concept. When the irradiance changes, the proposed algorithm produces an average η_{MPPT} of nearly 3.1% greater than that of the conventional P&O algorithm and the incremental conductance (InC) algorithm. In addition, under strong partial shading conditions and drift avoidance tests, the proposed algorithm produces an average η_{MPPT} of nearly 9% and 8% greater than that of the conventional algorithms, respectively.**

***Index Terms*—Photovoltaic system, maximum power point tracking (MPPT), perturb and observe (P&O), boost converter, steady-state performance.**

I. Introduction

SOLAR photovoltaic (PV) is predicted to be one of the most popular renewables due to its availability, ease of installation, and near-zero maintenance. PV power generation systems are used to convert solar energy to electricity. However, PV power fluctuates depending on the irradiation and temperature. Therefore, solar electricity is still more expensive than fossil fuels due to the low conversion efficiency of PV modules.

Designing an effective control algorithm plays a vital role in developing an efficient PV system [1]. In PV systems, it is well known that one of the main solutions to increasing efficiency is the application of the maximum power point tracking (MPPT) algorithms [2]. Because the MPPT is made up of software codes, it appears to be the most cost-effective solution to increasing energy throughput. MPPT ensures that the operating voltage and current remain at the maximum power point (MPP) on the *P*-*V* characteristic curve at all time [3].

There are many research papers with a variety of control techniques for PV MPPT systems. They are mainly divided into two categories: conventional and soft computing algorithms. Several studies have been carried out on conventional MPPT algorithms such as perturb and observe (P&O) algorithms [4]-[6], incremental conductance (InC) algorithm [7], [8], and hill-climbing (HC) algorithm [9], [10]. Conventional MPPT algorithms are the most commonly used due to their ease of implementation, as a result of which they have become more suitable for low-cost applications. Despite their ease of use, conventional algorithms have demonstrated a sluggish response to the changes in ambient temperature and solar radiation power. Consequently, the deviation of the system from its MPP results in a power loss that is proportional to the size of the installed PV array [1].

Besides conventional algorithms, there are many other solutions such as bioinspired algorithms, which are much more efficient in some special cases compared with conventional ones. They are capable enough to quickly converge to a global maximum and hence can save power loss even in a partially shaded environment [11]. Particle swarm optimization (PSO) is a bioinspired algorithm that is employed successfully in [12]. A genetic algorithm (GA) is such an algorithm that solves the obstacle of partial shading [13], [14]. Moreover, there are two artificial intelligence (AI) based algorithms, i.e., fuzzy logic-based controllers (FLBCs) and artificial neural network (ANN)-based MPPT [15], [16]. Although the mentioned algorithms show less settling time, less overshoot, and better performance about MPPT, they require data set at the beginning to train the input-output relation. In [17] and [18], sliding mode and Lyapunov function-

Manuscript received: April 27, 2022; revised: July 27, 2022; accepted: September 13, 2022. Date of CrossCheck: September 13, 2022. Date of online publication: October 28, 2022.

This article is distributed under the terms of the Creative Commons Attribution 4.0 International License (http://creativecommons.org/licenses/by/4.0/).

R. Kahani (corresponding author), M. Jamil, and M. T. Iqbal are with the Department of Electrical and Computer Engineering, Memorial University of Newfoundland, St. John's, A1B 3X5, Canada (e-mail: r.kahani@mun.ca; mjamil@mun.ca; tariq@mun.ca).

DOI: 10.35833/MPCE.2022.000245

based algorithms are presented for achieving MPPT control of a PV array tied with the power grid. In addition, nonlinear optimal feedback control is employed in [1] to deal with the oscillations around the MPP of the system. Although there exist various techniques in the literature that try to improve the drawbacks of conventional MPPT algorithms, they are substantially slower, and the implementation is still in priority when the control methods are put into practice. Therefore, the modified conventional MPPT algorithms are more popular algorithm to apply instead of the complicated modern theories. P&O algorithm is the simplest among the conventional MPPT algorithms and has excellent convergence. The algorithm, however, has two significant flaws. The first is the constant oscillation that happens in the vicinity of the MPP. Second, when the irradiance increases rapidly or when the irradiance is non-uniform (i.e., PSC), the P&O algorithm is prone to losing its tracking orientation. Both issues contribute to power loss and, as a result, a reduction in tracking efficiency. As the fluctuation around the MPP is the source of power loss, there are many research works trying to modify the conventional MPPT algorithms in the case of PSC [19]-[22] and drift avoidance issues [23], [24]. Complex computations and large memory requirements are the drawbacks of the mentioned research works. Moreover, they are not multi-purpose solutions and only consider specific issues of conventional algorithms. This paper offers a new modified P&O algorithm to compensate for the steady-state oscillation of MPPT. This algorithm presents a new method to recognize the peak power point when the stable condition arrives at the maximum of the output power of PV array. In this way, when the current and voltage of the PV array reach the optimum point, the duty cycle will remain constant, and no chattering will be produced around MPP. The conventional and modified P&O algorithms are thoroughly benchmarked in this paper under varying environmental conditions utilizing the steady state and dynamic MPPT efficiency tests, PSC tests, and drift effect tests. Those tests require the algorithm to track irradiance ramps with varying rates of change. Also, the modified P&O algorithm compares with the InC algorithm. The performance boost from the suggested algorithm is clarified when the results for the conventional algorithms and modified P&O algorithm have been compared under all mentioned environmental conditions. In this way, the proposed algorithm can be considered a multi-purpose solution under crucial MPPT conditions.

II. Problem Statement

A. PV Array Model

An electrical equivalent model of PV array is given in Fig. 1 for a PV system with parallel branch of the PV module N_s and series branch of the PV module N_p linked in series-parallel. In Fig. 1, I is the output current of the PV array; V is the output voltage of the PV array; I_{ph} is the light generated current; I_{sh} is the shunt resistor current; and R_{sh} and R_s are the shunt and series resistances of the PV module, respectively.

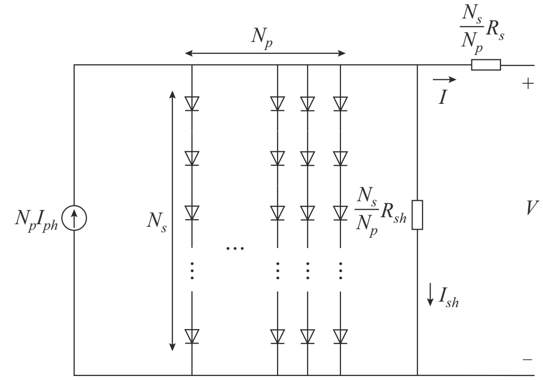

Fig. 1. Electrical equivalent model of PV array.

By considering Kirchhoff's current law, the output current of the PV module is equal to:

$$I=N_pI_{ph}-N_pI_s\left(\exp\left(\frac{\frac{R_sI}{N_p}+\frac{V}{N_s}}{nV_T}\right)-1\right)-I_{sh} \tag{1}$$

where n and V_T are the ideality factor and thermal voltage of the PV module, respectively. Moreover, considering R_{sh} and R_s of the PV module in the circuit, we can find the current flowing through the shunt resistor:

$$I_{sh}=\frac{R_sI+\frac{N_p}{N_s}V}{R_{sh}} \tag{2}$$

For simplification, assume that $R_s << R_{sh}$. Considering the model values $R_s=0$ and $R_{sh}=\infty$, (1) will be determined as:

$$I=N_pI_{ph}-N_pI_s\left(\exp\left(\frac{V}{nN_sV_T}\right)-1\right) \tag{3}$$

Therefore, the output voltage of the PV array can be calculated as:

$$V=N_snV_T\ln\left(\frac{N_pI_{ph}+N_pI_s-I-I_{sh}}{N_pI_s}\right) \tag{4}$$

B. DC-DC Boost Converter

A converter is the main part of the MPPT controller of the PV array, which helps to match the impedance observed from the PV device and that observed from the load side. Therefore, the output voltage of PV will change according to the adjusted impedance. Many DC-DC converter topologies have been studied, such as the boost topology [25], [26], buck topology, buck-boost converter topology, and single-ended primary inductor converter (SEPIC) topology [27], [28]. The boost converters are involved in increasing the voltage. The buck converters are applied to lower the voltage. Then, the buck-boost converters and SEPICs are competent to step up and step down the output voltage. There are also lots of studies that compare the different types of converter performance. In [25], step-up DC-DC converters in various configurations are proposed. Reference [29] analyzes boost converters and SEPICs considering output voltage ripple, total harmonic distortion, and power factor for both converters, and boost converters produce better results. Besides the mentioned features, boost converters are easier to use. Therefore, the boost-type converter is frequently used because of its superior performance. For the characteristics discussed earlier, we select the boost topology to place between PV array and load. As illustrated in Fig. 2, the main elements of a boost converter are the inductor L, diode, capacitors C_1 and C_2, and switch. In this paper, we use MOSFET as a switch that can be turned on and off consistently based on the generated duty cycle. The variability in the PV voltage control process is caused by the dynamic resistance, which is obtained from the slope of its *I-V* curve [30], [31]. This parameter depends on the characteristics of the PV array and is highly variable with the irradiation, the temperature, and especially the PV voltage. As a result, the voltage regulation performance can be diminished when operating under MPPT because of the irradiation and temperature change [32].

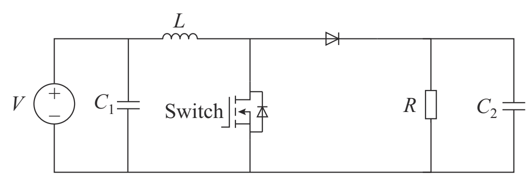

Fig. 2. Equivalent circuit of boost converter.

The dynamic model of the boost converter circuit is:

$$\begin{cases} \dfrac{\mathrm{d}V}{\mathrm{d}t} = \dfrac{1}{C_1}(I - I_L) \\ \dfrac{\mathrm{d}I_L}{\mathrm{d}t} = \dfrac{1}{L}\left(V + \dfrac{D-1}{L}V_{out}\right) \\ \dfrac{\mathrm{d}V_{out}}{\mathrm{d}t} = \dfrac{1}{C_2}(I_L - I_{out}) + \dfrac{1}{C_2}DI_L \end{cases} \tag{5}$$

where D is the duty cycle of the waveform driving the switch; I_L is the current of the DC-DC converter inductor; and I_{out} and V_{out} are the desired output current and voltage of the DC-DC converter, respectively. Then, we can obtain:

$$\dot{\boldsymbol{x}} = \boldsymbol{f}(\boldsymbol{x}) + \boldsymbol{g}(\boldsymbol{x})D \tag{6}$$

$$\begin{cases} \boldsymbol{x} = \begin{bmatrix} V \\ I_L \\ V_{out} \end{bmatrix} \\ \boldsymbol{f}(\boldsymbol{x}) = \begin{bmatrix} \dfrac{1}{C_1}(I - I_L) \\ \dfrac{1}{L}(V - V_{out}) \\ \dfrac{1}{C_2}(I_L - I_{out}) \end{bmatrix} \\ \boldsymbol{g}(\boldsymbol{x}) = \begin{bmatrix} 0 \\ \dfrac{1}{L}V_{out} \\ -\dfrac{1}{C_2}I_L \end{bmatrix} \end{cases} \tag{7}$$

In continuous conduction mode (CCM), the following equation relates the output voltage to the input voltage [33]:

$$V_{out} = \frac{1}{1-D}V \tag{8}$$

$$P = P_{out} \tag{9}$$

Based on (9), it is easy to extract that:

$$R_{out} = R_{pv}\frac{1}{(1-D)^2} \tag{10}$$

where R_{pv} is the PV panel load and it is also the input load of the boost converter.

Equation (10), which is based on the equation $R_{pv} = R_{out}(1-D)^2$, shows that if D decreases or increases, R_{pv} increases or decreases; consequently, based on the *I-V* characteristic, the current of the panel will increase, and the voltage of the panel will decrease. Equivalently, as the voltage decreases or increases, the current increases or decreases, as shown in (4).

This demonstrates that the rate at which the duty cycle changes is always the inverse of the voltage change rate. This can be mathematically expressed as:

$$\mathrm{sign}(\dot{V}) = -\mathrm{sign}(\dot{D}) \tag{11}$$

The output power of a PV generator is given by $P = VI$. The power optimization is done by forcing the system to operate at a certain point, which is defined by solving (12).

$$\frac{\mathrm{d}P}{\mathrm{d}V} = 0 \tag{12}$$

III. Proposed P&O Algorithm

A. Overview of P&O Algorithm

The P&O algorithm is based on perturbing the PV array output voltage by tuning the duty cycle (perturbation step-size) of a power converter and then checking the changes in the output power of the array. If ΔP is positive, it means we are approaching the maximum panel power, and the perturbation must be made in the same direction. Conversely, if the output power decreases, the perturbation must be made in the reverse order. $\Delta P = 0$ shows that the MPP is reached. The flowchart of conventional P&O algorithm is shown in Fig. 3, where k denotes the interval.

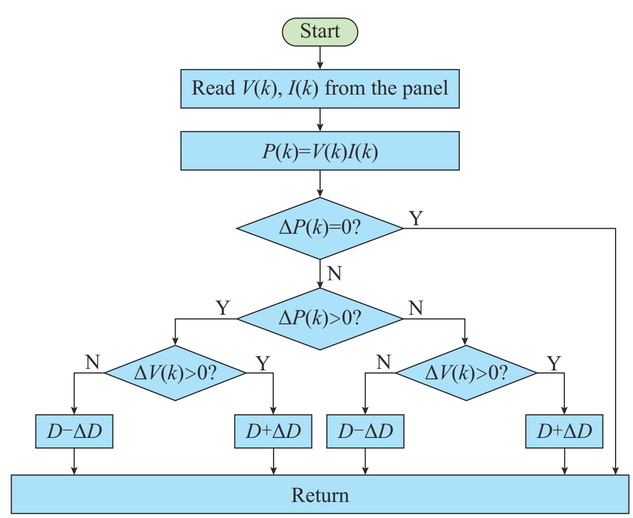

Fig. 3. Flowchart of conventional P&O algorithm.

The perturbation step size plays an undeniable role in reaching the MPP as the large step size may lead to a fast-tracking response, but the amplitude of the steady-state oscillations will be high. Besides, if the step size has a small value, the tracking is slower, and still, a small oscillation will be observed. Nonstop oscillation around the MPP is the main drawback of the P&O algorithm. Unfortunately, this hindrance is bold because it leads to energy losses.

B. Proposed P&O Algorithm

The proposed algorithm focuses on the steady-state response of PV array power output. As the oscillation around the MPP is the source of power loss, we have to reduce the fluctuation as much as possible. It is evident in Fig. 3 that the only case that the original P&O algorithm stops oscillation is when $\Delta P=0$. For the other issues, the fluctuation around the MPP is inevitable. As the $\Delta P=0$ rarely occurs during the perturbation, we need to increase the chance of stopping the oscillation when the output power is extremely close to the climax of the power curve. For this proposal, one parameter is added to the MPPT flowchart, which is $\Delta P(k-1)>0$ to recognize when the algorithm is crossing the MPP of the power curve. In this way, the sign of $\Delta P(k)$ in each cycle will be compared with the sign of $\Delta P(k-1)>0$, that is equal to ΔP in the previous cycle. If these two signs are different, it means the PV array output power crosses the MPP, and the duty cycle should not be changed. In other words, if the perturbation makes a decrease or increase in array terminal power after an increase or decrease in the preceding cycle, it means we are crossing the MPP of the power curve, so the duty cycle of the boost converter should remain the same as the previous cycle. In this manner, the steady-state oscillation will be eliminated in case of constant illumination. The flowchart of the proposed P&O algorithm is shown in Fig. 4.

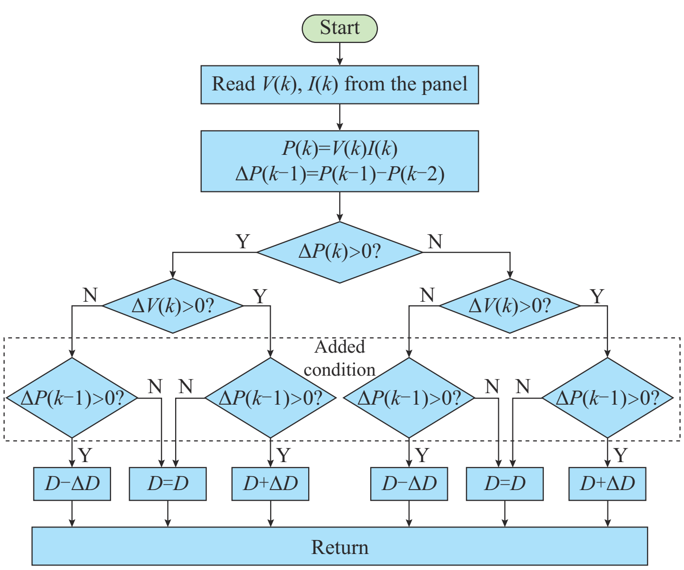

Fig. 4. Flowchart of proposed P&O algorithm.

A positive scalar function of the state variables of the system is picked out as:

$$E=\frac{1}{2}S^2>0 \tag{13}$$

$$S=\frac{\mathrm{d}P}{\mathrm{d}V}=I+\frac{\mathrm{d}I}{\mathrm{d}V}V \tag{14}$$

Then, the following condition is the sufficient condition for the global stability of the system.

$$\dot{E}=S\frac{\mathrm{d}S}{\mathrm{d}t}<0_s \quad \dot{S}S<0 \tag{15}$$

where $\dot{S}$ is the derivative of S.

Using (3), we can obtain:

$$S=\frac{\mathrm{d}P}{\mathrm{d}V}=N_pI_{ph}-N_pI_s\left(\exp\left(\frac{V}{nN_sV_T}\right)-1\right)-\frac{N_pI_s}{nN_sV_T}\exp\left(\frac{V}{nN_sV_T}\right) \tag{16}$$

When $S=0$, the PV system has reached its maximum output. As a result, the dynamics of the system can be split into two states: $S<0$ and $S>0$.

When $S<0$, the proposed algorithm is divided into two types of situations: $\Delta P(k-1)>0$ and $\Delta P(k-1)<0$.

If $\Delta P(k-1)>0$, the proposed algorithm treats the same as the PV system reaches the MPP, so the oscillation will be removed. If $\Delta P(k-1)<0$, based on the proposed algorithm, $\dot{D}>0$ and by using (7), $\dot{V}$ decreases:

$$\dot{V}<0 \tag{17}$$

As we know, the derivative of S is:

$$\dot{S}=\frac{\mathrm{d}S}{\mathrm{d}V}\dot{V} \tag{18}$$

Then, using (12), we can obtain:

$$\dot{S}=-\frac{N_pI_s}{nN_sV_T}\left(\exp\left(\frac{V}{nN_sV_T}\right)+\left(1+\frac{1}{nN_sV_T}\right)\exp\left(\frac{V}{nN_sV_T}\right)\right)\dot{V} \tag{19}$$

Substituting (14) in (16) results in $\dot{S}>0$, thus we can obtain:

$$\dot{S}S<0 \tag{20}$$

When $S>0$, the proposed algorithm is divided into two different situations $\Delta P(k-1)>0$ and $\Delta P(k-1)<0$.

If $\Delta P(k-1)<0$, the proposed algorithm treats the same as the PV system reaches the MPP. If $\Delta P(k-1)>0$, based on the proposed algorithm, $\dot{D}<0$, and by using (8), V increases:

$$\dot{V}>0 \tag{21}$$

Substituting (18) in (16) results in $\dot{S}<0$, thus we can obtain (20). Overall, the PV system is globally stable.

C. Proposed P&O Algorithm with Optimized Duty Cycle

In this subsection, a slight change in the proposed algorithm results in a big difference in tracking efficiency. The step size of the proposed algorithm should be flexible by getting close to the MPP. It means that each algorithm is closer to the MPP, and the step size should be smaller. Therefore, the proposed algorithm has the chance to stop as close as possible to the maximum power curve.

When the proposed algorithm approaches the MPP to the right, the rate of approaching the MPP is optimized by multiplying the duty cycle by a coefficient that is directly proportional to the voltage of PV module and inversely proportional to the current, and it is directly proportional to the current and inversely proportional to the voltage when approaching the MPP to the left. Because the step size of the algorithm reduces as it gets closer to the MPP, it helps the algorithm track the MPP more precisely. Therefore, the equations of changing the duty cycle $D=D-\Delta D$ and $D=D+\Delta D$ have to be replaced by $D=D-(I/V)\Delta D$ and $D=D+(I/V)\Delta D$, respectively.

IV. Simulation Results

This section performs a simulation on MATLAB/Simulink, which is prepared to indicate the performance of the proposed algorithm. We used Trina Solar TSM-250PA05.08 in 4 parallel strings with 10 modules connected in series per string. Table I shows the electrical data of the selected solar panel TSM 250PA05.08. The components of the boost converter are picked according to the values recommended in Table II.

TABLE I
Electrical Data of Selected Solar Panel

Electrical data under standard test conditions	Value
Peak power P_{max}	250 W
Production tax credit rating	227.5 W
Power output tolerance	0, +3%
Voltage (the maximum power)	30.3 V
Current (the maximum power)	8.27 A
Open-circuit voltage	37.6 V
Short-circuit current	8.85 A
Module efficiency	15.3%

A. Case 1: Proposed P&O Algorithm

1) Performance of Sudden Irradiance Level Change Tracking

To confirm the performance of the proposed P&O algorithm, a profile of the solar irradiation is used, which contains both step-up and step-down shapes. The irradiance values are between 700 W/m^2 and 800 W/m^2. The illumination profile is illustrated in Fig. 5. The irradiance starts from 720 W/m^2, lasts for 0.6 s at this level; then steps up to 760 W/m^2, remains at this level for 0.8 s; then steps down to 700 W/m^2, stays flat for 0.6 s. As we focus on steady-state conditions in the proposed algorithm, the step up or step down is not considered in the irradiance profile. The simulation time is 2 s, and the temperature is retained at a fixed value of 25 °C.

TABLE II
Components of Boost Converter

Component	Value
Inductor	50 μH
Capacitor	2 mF
Voltage (the maximum power)	870 V
Switching frequency	5 kHz

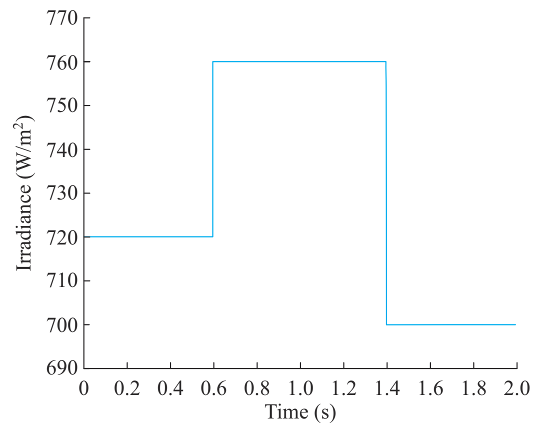

Fig. 5. Illumination profile.

Figure 6 shows the comparison of tracking performances of the conventional P&O algorithm and the proposed P&O algorithm at varying irradiance levels. It is apparent in the enlarged images in Fig. 6 that the tracking deviation in the proposed P&O algorithm is minimal.

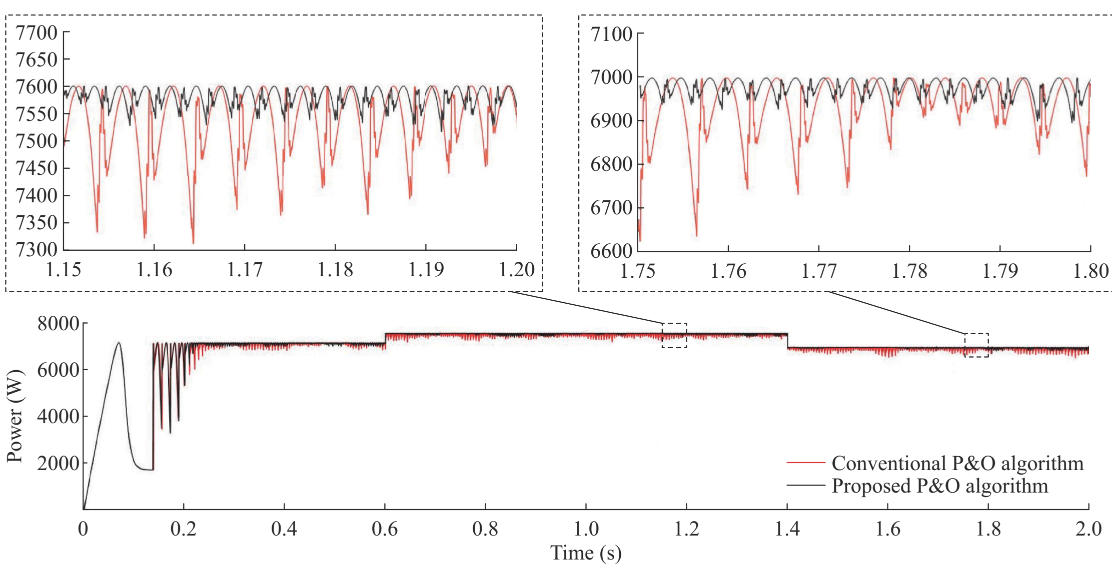

Fig. 6. Comparison of tracking performances of conventional P&O algorithm and proposed P&O algorithm at varying irradiance levels.

Another simulation is done to emphasize the performance of the proposed algorithm. Figure 7 depicts a comparison of tracking performances of proposed P&O algorithm and InC MPPT at varying irradiance levels. It is found that the propsoed P&O algorithm is more oscillation-free than the InC MPPT.

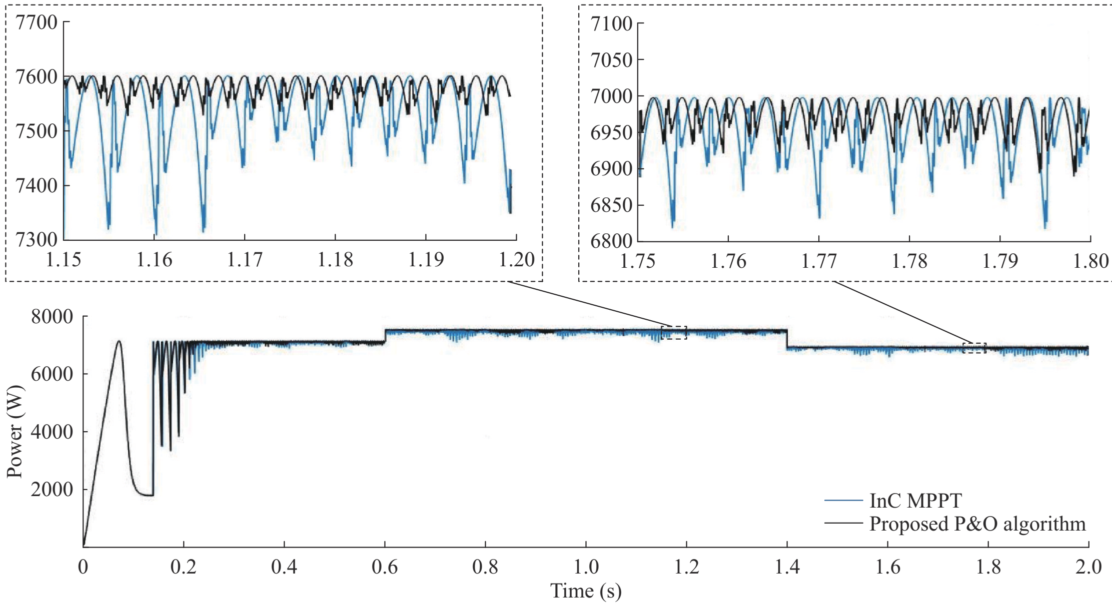

Fig. 7. Comparison of tracking performances of proposed P&O algorithm and InC MPPT at varying irradiance levels.

The average efficiency of MPPT algorithm is measured using the MPPT efficiency formula:

$$\eta_{MPPT,avg}=\frac{\int P_{out}(t)\mathrm{d}t}{\int P_{\max}(t)\mathrm{d}t} \tag{22}$$

The power-voltage plot for 10 Trina modules connected in series per string is illustrated in Fig. 8.

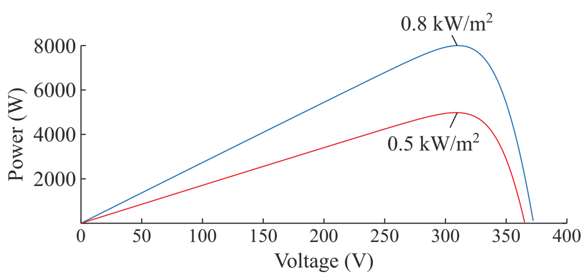

Fig 8. Power-voltage plot for 10 Trina modules per series string.

It is shown in Fig. 8 that the maximum power production for 0.8 kW/m^2 is 8000 W, and the maximum power production for 0.5 kW/m^2 is 5000 W. Now, by adding the maximum power that can be produced per sample time (2 μs) for the determined illustration profiles in Fig. 5, we can obtain the integration of the maximum power (denominator of (22)) for the whole simulation time (2 s). The numerator of the efficiency equation (22) will be calculated by adding the power generated by the whole modules per sample time. We can easily measure the efficiency of the MPPT algorithm by dividing two calculated amounts.

As a result, the tracking efficiencies for each MPPT are determined. After the simulation investigation, the test results of sudden irradiance level change are presented in Table III.

TABLE III
TEST RESULTS OF SUDDEN IRRADIANCE LEVEL CHANGE

Algorithm	Evaluated parameter	
	Nature of tracking waveforms	Tracking efficiency (%)
Proposed P&O	Less oscillatory and stable	95.27
Conventional P&O	Oscillatory	93.52
InC MPPT	Oscillatory	93.67

2) Test of Dynamic MPPT Efficiency

In this subsection, two different ranges of irradiance change, i.e., slow and fast, cover the dynamic MPPT efficiency of the proposed P&O algorithm. The slow insolation change is 20 W/m^2 from 700 W/m^2 to 720 W/m^2, and the fast insolation change is 50 W/m^2 from 700 W/m^2 to 750 W/m^2.

Figures 9 and 10 show the tracking performances of both the conventional and proposed P&O algorithms. Certain waveform parts are enlarged for clarity. The tracking by the proposed P&O algorithm is almost perfect at the very slow insolation change (20 W/m^2), as shown in the magnified axes. This is due to the fact that the gradual ramp resembles a steady-state scenario in which the variable perturbation sizing is turned on.

The conventional P&O algorithm, on the other hand, exhibits significant oscillation due to the huge and fixed perturbation size.

However, because it can cope with the (slow) shift in irradiance, there is no evident loss of tracking direction. Similar results are obtained by the fast irradiance change.

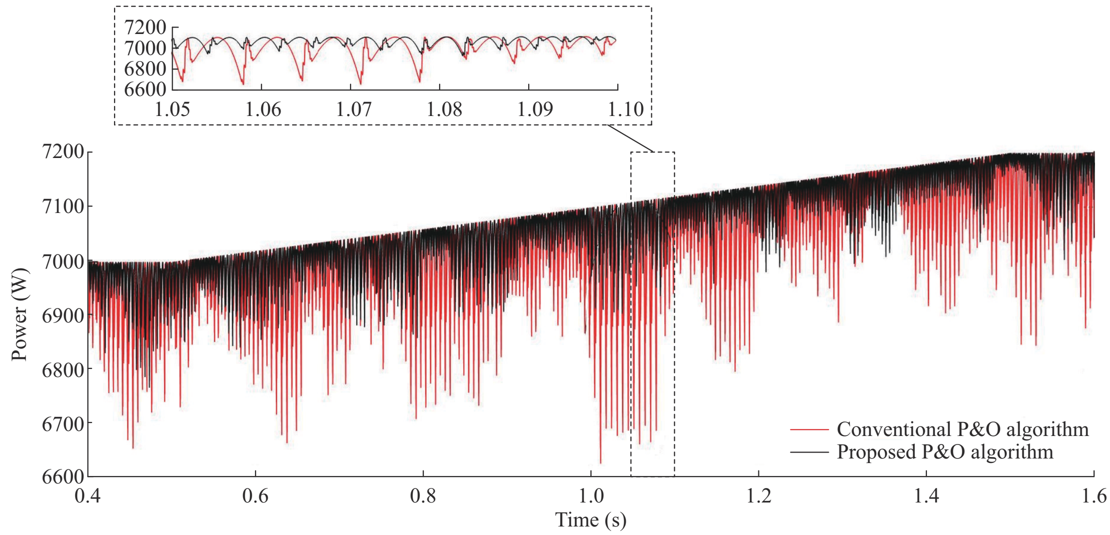

Fig. 9. Comparison of tracking performances of conventional P&O algorithm and proposed P&O algorithm at slow irradiance change.

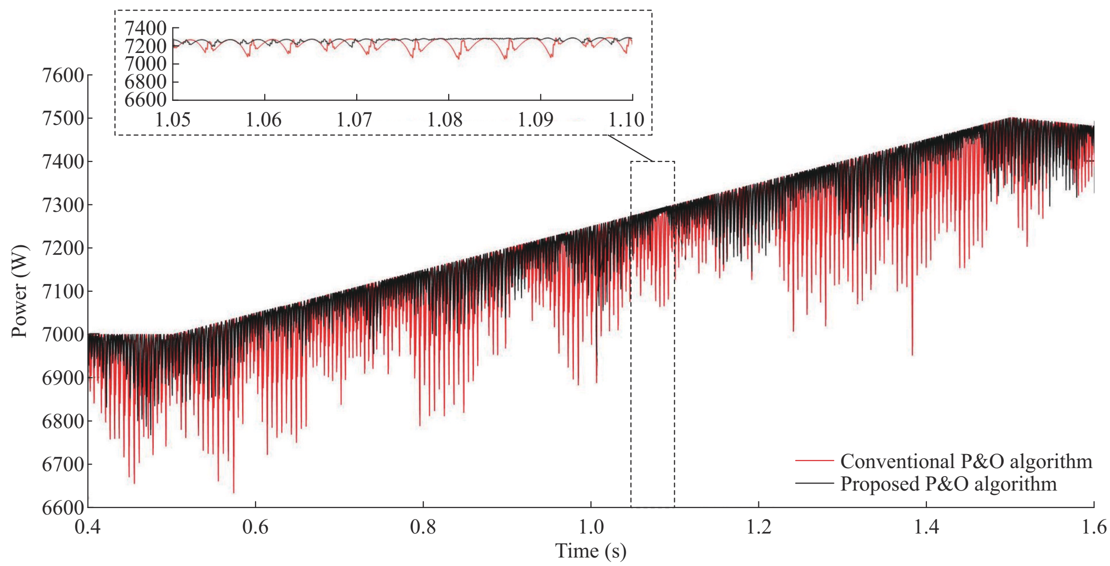

Fig. 10. Comparison of tracking performances of conventional P&O algorithm and proposed P&O algorithm at fast irradiance change.

Based on mentioned tests of dynamic irradiance change, the proposed algorithm achieves $\eta_{MPPT,avg}$ of almost 0.5% higher than the conventional P&O algorithm in both slow and fast irradiance change. Besides, the tracking performance of the proposed P&O algorithm is highly constant.

Table IV shows the test results of dynamic irradiance change. The values of $\eta_{MPPT,avg}$ for the conventional P&O algorithm and the proposed P&O algorithm in the slow ramp zone (20 W/m^2 per second) are 96.19% and 96.68%, respectively.

TABLE IV
TEST RESULTS OF DYNAMIC IRRADIANCE CHANGE

Algorithm	Evaluated parameter	
	Slow irradiance change tracking efficiency (%)	Fast irradiance change tracking efficiency (%)
Proposed P&O	96.68	96.72
Conventional P&O	96.19	96.23

When the insolation changes quickly (50 W/m^2 per second), the efficiencies of the conventional P&O algorithm and the proposed P&O algorithm are 96.23% and 96.72%, respectively.

B. Case 2: Proposed P&O Algorithm with Optimized Duty Cycle

In this case, the rate of approaching the MPP is optimized by multiplying the duty cycle by a coefficient that is directly proportional to the voltage of the PV module and inversely proportional to the current when approaching the MPP to the right; and it is directly proportional to the current of the PV module and inversely proportional to the voltage when approaching the MPP to the left. It aids the algorithm in tracking the MPP more precisely since the step size of the algorithm decreases as it gets closer to the MPP. The suggested extended MPPT technique is tested in simulations and experiments to ensure that it can deliver a satisfactory dynamic response and steady-state performance for a PV power generation system. The comparison of tracking performances of proposed P&O algorithm and conventional P&O algorithm at varying irradiance levels is shown in Fig. 11. Based on simulation results, the proposed algorithm obtains $\eta_{MPPT,avg}$ of almost 3.14% greater than that of the conventional P&O algorithm.

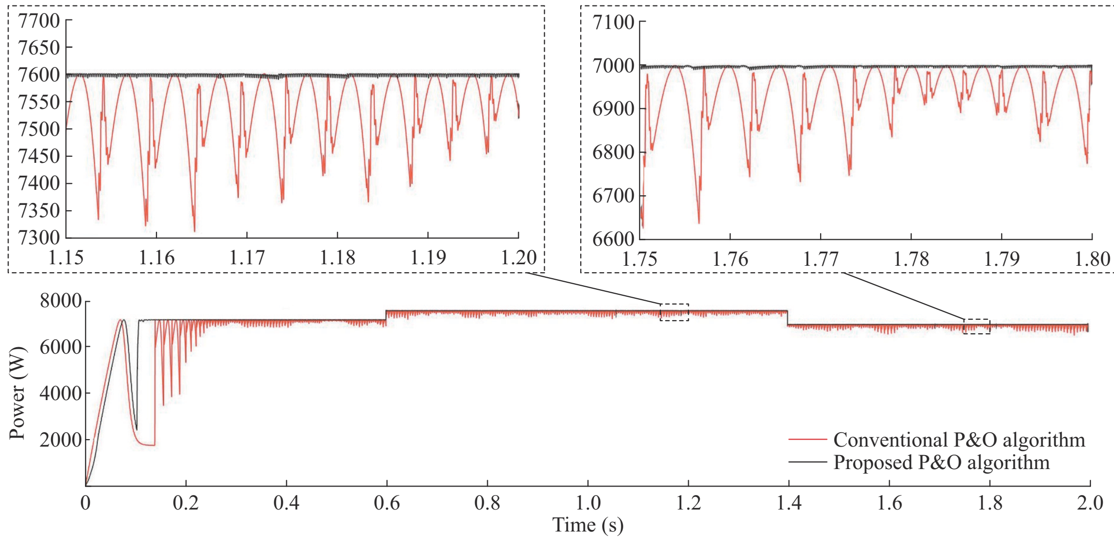

Fig. 11. Comparison of tracking performances of proposed P&O algorithm and conventional P&O algorithm at varying irradiance levels.

Another simulation is done to emphasize the performance of the proposed algorithm with an optimized duty cycle. Figure 12 shows a comparison of tracking performances of proposed P&O algorithm and InC MPPT at varying irradiance levels. It is found that the proposed P&O algorithm is more oscillation-free than the InC MPPT. The proposed algorithm obtains $\eta_{MPPT,avg}$ of almost 3.13% greater than that of the InC MPPT.

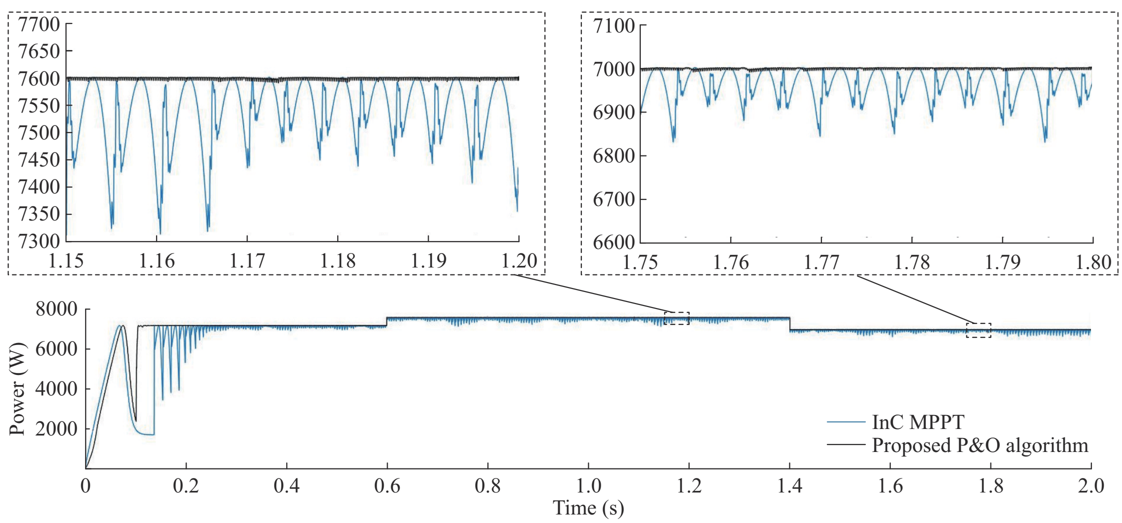

Fig. 12. Comparison of tracking performances of proposed P&O algorithm and InC MPPT at varying irradiance levels.

As a result, the tracking efficiencies for each MPPT are determined. After the simulation investigation, the test results of optimized duty cycle are shown in Table V.

TABLE V
TEST RESULTS OF OPTIMIZED DUTY CYCLE

Algorithm	Evaluated parameter	
	Nature of tracking waveforms	Tracking efficiency (%)
Proposed P&O	Less oscillatory and stable	98.21
Conventional P&O	Oscillatory	95.07
InC MPPT	Oscillatory	95.08

C. Case 3: Partial Shading Condition Test for Proposed P&O Algorithm with Optimized Duty Cycle

1) Moderate Partial Shading Pattern

In order to test the performance of the suggested MPPT controller at non-uniform irradiance levels, three parallel strings with five modules connected in series per string applied. Five PV modules that are not shaded receive 700 W/m^2 uniform irradiance, five partially shaded modules receive 300 W/m^2, and the five remaining modules receive 100 W/m^2 uniform irradiance.

Based on the simulation results, the proposed P&O algorithm obtains $\eta_{MPPT,avg}$ of almost 3.11% greater than the conventional P&O algorithm and InC MPPT. The test results of moderate PSCs are shown in Table VI.

TABLE VI
TEST RESULTS OF MODERATE PSCS

Algorithm	Evaluated parameter	
	Nature of tracking waveforms	Tracking efficiency (%)
Proposed P&O	Less oscillatory and stable	98.22
Conventional P&O	Oscillatory	95.11
InC MPPT	Oscillatory	95.11

2) Strong Partial Shading Pattern

In this case, five connected panels receive 750 W/m^2 radiation under uniform radiation conditions, while five receive 150 W/m^2 radiation and five receive 100 W/m2 radiation. The comparisons of tracking performances of proposed P&O algorithm and conventional P&O algorithm as well as the proposed P&O algorithm and InC MPPT under partial shading condition are shown in Figs. 13 and 14. Based on simulation results, the proposed algorithm obtains $\eta_{MPPT,avg}$ of almost 9.06% greater than the conventional P&O algorithm.

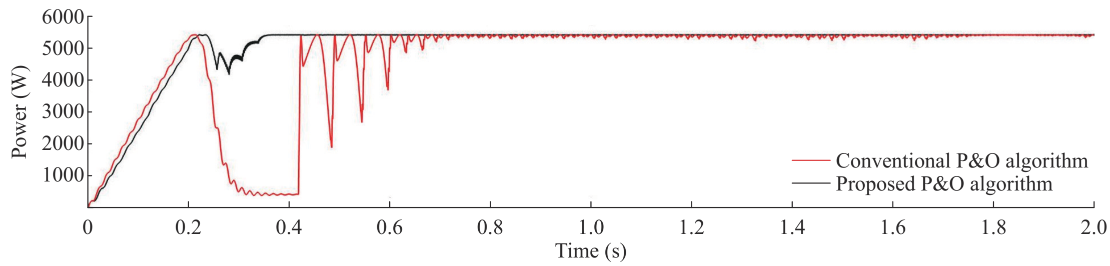

Fig. 13. Comparison of tracking performances of proposed P&O algorithm and conventional P&O algorithm under partial shading condition.

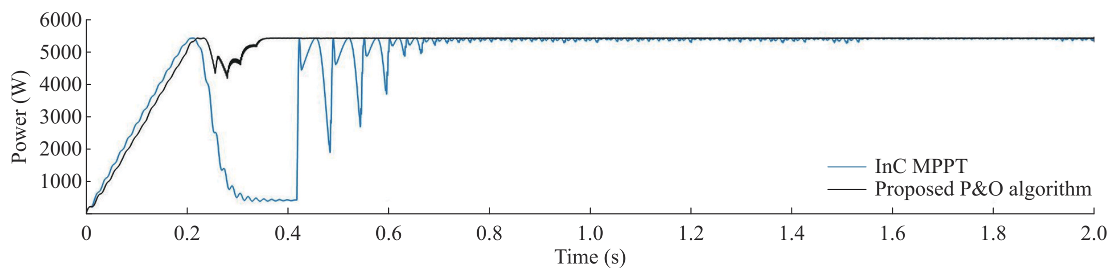

Fig. 14. Comparison of tracking performances of proposed P&O algorithm and InC MPPT under partial shading condition.

Another simulation is done to emphasize the performance of the proposed algorithm with an optimized duty cycle. It is found that the proposed P&O algorithm is more oscillation free than the InC MPPT. Also, the proposed algorithm obtains an average η_{MPPT} of almost 8.98% greater than the InC MPPT. The test results of strong PSCs are shown in Table VII.

TABLE VII
TEST RESULTS OF STRONG PSCS

Method	Evaluated parameter	
	Nature of tracking waveforms	Tracking efficiency (%)
Proposed P&O	Less oscillatory and stable	91.85
Conventional P&O	Oscillatory	82.79
InC MPPT	Oscillatory	82.87

As a comparison to the other P&O algorithms, the best efficiency among the partial shading patterns in [34] is 2% greater than the conventional P&O algorithm.

D. Case 4: Drift Analysis for One Step Change in Insulation

The tests of the proposed algorithm have been conducted for an insolation-level step shift from 300 to 700 W/m^2 in 0.1 s. This rapid change in insulation can be considered as a drift issue and is popular on cloudy days. The proposed algorithm can recognize whether the power increase is due to perturbation or an increase in insulation. The results of the drift test are shown in Table VIII.

TABLE VIII
RESULTS OF DRIFT TEST

Algorithm	Evaluated parameter	
	Nature of tracking waveforms	Tracking efficiency (%)
Proposed P&O	Less oscillatory and stable	93.83
Conventional P&O	Oscillatory	85.43
InC MPPT	Oscillatory	85.50

E. Case 5: Efficiency Test of Proposed P&O Algorithm According to EN 50530 Standard

The efficiency test of EN 50530 standard is used to evaluate the proposed algorithm under dynamic weather conditions. The solar insolation is supplied in a trapezoidal waveform with various ramp inclinations for the efficiency test of EN 50530 standard.

The irradiance variation ramps from x% to y% under standard test conditions (STCs), and the dynamic change at insulation level is shown in Fig. 15. Step time t_0 to t_4 is defined in Table IX.

The average dynamic MPPT efficiency is calculated based on (23). A summary of the test results of dynamic MPPT efficiency for the two types of sequence ramps, 10%-50% and 30%-100%, can be observed in Table IX.

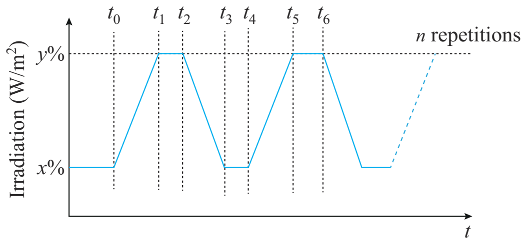

Fig. 15. Dynamic change at insulation level.

TABLE IX
TEST RESULTS OF DYNAMIC MPPT EFFICIENCY

Type of ramps	Step time (s)				Tracking efficiency (%)		
	t_1	t_2	t_3	t_4	Proposed P&O	Conventional P&O	InC MPPT
10%-50% ramp	0.1	0.4	0.1	0.4	77.67	52.97	52.97
	0.2	0.3	0.2	0.3	81.06	52.32	52.32
30%-100% ramp	0.1	0.4	0.1	0.4	95.29	89.21	89.44
	0.2	0.3	0.2	0.3	96.23	89.57	89.74

V. CONCLUSION

In this paper, the tracking efficiency of PV power output has been studied using MATLAB/Simulink. The strategy aims to reduce steady-state oscillation while minimizing the loss due to the losing direction. A proposed P&O algorithm is presented to eliminate the oscillation of PV power around the peak point. The algorithm is able to properly identify oscillation and add a boundary condition that prevents it from diverging from the MPP. Besides, the optimized duty cycle helps the algorithm to follow the MPPT by adjustable step sizes. By implementing the proposed P&O algorithm, the average η_{MPPT} improves by nearly 3.1% greater than the conventional P&O algorithm and the InC MPPT during sudden irradiance changes. Moreover, the proposed P&O algorithm performs better than the conventional P&O algorithm under dynamic irradiance changes by enhancing the efficiency by 0.5% under the slow and fast irradiance changes. In addition, under strong partial shading conditions and drift avoidance tests, the proposed algorithm produces an average η_{MPPT} of nearly 9% and 8% greater than the conventional P&O algorithms. By considering the results, it is confirmed that the proposed P&O algorithm could track the irradiance profile with a minor deviation from MPPs under various environmental changes. Therefore, more power loss is prevented, and the tracking accuracy is increased.

Because the proposed P&O algorithm is the modified version of the conventional algorithm, the implementation is simple as well. In the future, we aim to improve the algorithm for fast convergence at the operating point.

REFERENCES

[1] M. Farsi and J. Liu, "Nonlinear optimal feedback control and stability analysis of solar photovoltaic systems," *IEEE Transactions on Control Systems Technology*, vol. 28, no. 6, pp. 2104-2119, Nov. 2020.

[2] E. I. Batzelis, G. E. Kampitsis, S. A. Papathanassiou *et al.*, "Direct MPP calculation in terms of the single-diode PV model parameters," *IEEE Transactions on Power Electronics*, vol. 30, no. 1, pp. 226-236, Mar. 2015.

[3] J. Ahmed and Z. Salam, "A modified P&O maximum power point tracking method with reduced steady-state oscillation and improved tracking efficiency," *IEEE Transactions on Sustainable Energy*, vol. 7, no. 4, pp. 1506-1515, Oct. 2016.

[4] N. Femia, G. Petrone, G. Spagnuolo *et al.*, "Optimization of perturb and observe maximum power point tracking method," *IEEE Transactions on Power Electronics*, vol. 20, no. 4, pp. 963-973, Jul. 2005.

[5] H. A. Sher, A. F. Murtaza, A. Noman *et al.*, "A new sensorless hybrid MPPT algorithm based on fractional short-circuit current measurement and P&PO MPPT," *IEEE Transactions on Sustainable Energy*, vol. 6, no. 4, pp. 1426-1434, Oct. 2015.

[6] M. A. Elgendy, B. Zahawi, and D. J. Atkinson, "Assessment of perturb and observe MPPT algorithm implementation techniques for PV pumping applications," *IEEE Transactions on Sustainable Energy*, vol. 3, no. 1, pp. 21-33, Jan. 2012.

[7] J. H. Lee, H. Bae, and B. H. Cho, "Advanced incremental conductance MPPT algorithm with a variable step size," in *Proceedings of 12th International Power Electronics and Motion Control Conference*, Portoroz, Slovenia, Aug. 2006, pp. 603-607.

[8] Q. Mei, M. Shan, L. Liu *et al.*, "A novel improved variable step-size incremental-resistance MPPT method for PV systems," *IEEE Transactions on Industrial Electronics*, vol. 58, no. 6, pp. 2427-2434, Jun. 2011.

[9] W. Xiao and W. G. Dunford, "A modified adaptive hill climbing MPPT method for photovoltaic power systems," in *Proceedings of IEEE 35th Annual Power Electronics Specialists Conference*, Aachen, Germany, Jun. 2004, pp. 1957-1963.

[10] E. Koutroulis, K. Kalaitzakis, and N. C. Voulgaris, "Development of a microcontroller-based, photovoltaic maximum power point tracking control system," *IEEE Transactions on Power Electronics*, vol. 16, no. 1, pp. 46-54, Jan. 2001.

[11] R. Iftikhar, I. Ahmad, M. Arsalan *et al.*, "MPPT for photovoltaic system using nonlinear controller," *International Journal of Photoenergy*, vol. 2018, p. 6979723, Apr. 2018.

[12] F. M. de Oliveira, F. R. Durand, V. D. Bacon *et al.*, "Grid-tied photovoltaic system based on PSO MPPT technique with active power line conditioning," *IET Power Electronics*, vol. 9, no. 6, pp. 1180-1191, May 2016.

[13] M. B. Smida and A. Sakly, "Genetic based algorithm for maximum power point tracking (MPPT) for grid connected PV systems operating under partial shaded conditions," in *Proceedings of 7th International Conference on Modelling, Identification and Control (ICMIC)*, Sousse, Tunisia, Dec. 2015, pp. 1-6.

[14] A. A. S. Mohamed, A. Berzoy, and O. A. Mohammed, "Design and hardware implementation of FL-MPPT control of PV systems based on GA and small-signal analysis," *IEEE Transactions on Sustainable Energy*, vol. 8, no. 1, pp. 279-290, Jan. 2017.

[15] M. Dehghani, M. Taghipour, G. B. Gharehpetian *et al.*, "Optimized fuzzy controller for MPPT of grid-connected PV systems in rapidly changing atmospheric conditions," *Journal of Modern Power Systems and Clean Energy*, vol. 9, no. 2, pp. 376-383, Mar. 2021.

[16] R. Kumar, N. Tadikonda, J. Kumar *et al.*, "An ANN-based MPPT technique for partial shading photo voltaic distribution generation," in *Control Applications in Modern Power Systems.* Singapore: Springer, 2022, pp. 391-403.

[17] M. Rezkallah, S. K. Sharma, A. Chandra *et al.*, "Lyapunov function and sliding mode control approach for the solar-PV grid interface system," *IEEE Transactions on Industrial Electronics*, vol. 64, no. 1, pp. 785-795, Jan. 2017.

[18] S. Golzari, F. Rashidi, and H. F. Farahani, "A Lyapunov function-based model predictive control for three phase grid connected photovoltaic converters," *Solar Energy*, vol. 15, no. 181, pp. 222-233, Mar. 2019.

[19] S. Rezazadeh, A. Moradzadeh, and S. M. Hashemzadeh, "A novel prime numbers-based PV array reconfiguration solution to produce maximum energy under partial shade conditions," *Sustainable Energy Technologies and Assessments*, vol. 1, no. 47, p. 101498, Oct. 2021.

[20] M. Madhukumar, T. Suresh, and M. Jamil, "Investigation of PV integrated grid system under nonuniform irradiance conditions," *Electronics*, vol. 9, no. 9, p. 1512, Aug. 2020.

[21] S. M. Hashemzadeh, "A new model-based technique for fast and accurate tracking of global maximum power point in photovoltaic arrays

under partial shading conditions," *Renewable Energy*, vol. 1, no. 139, pp. 1061-76, Aug. 2019.

[22] V. K. Vethanayagam, K. K. Prabhakaran, and V. Balasubramanian, "A novel algorithm based on voltage and current perturbation to track global peak under partial shading conditions," *IEEE Transactions on Energy Conversion*, vol. 37, no. 4, pp. 2461-2471, May 2022.

[23] M. Killi and S. Samanta, "Modified perturb and observe MPPT algorithm for drift avoidance in photovoltaic systems," *IEEE Transactions on Industrial Electronics*, vol. 62, no. 9, pp. 5549-5559, Sept. 2015.

[24] V. Jately, S. Bhattacharya, B. Azzopardi *et al*., "Voltage and current reference based MPPT under rapidly changing irradiance and load resistance," *IEEE Transactions on Energy Conversion*, vol. 36, no. 3, pp. 2297-2309, Sept. 2021.

[25] M. Forouzesh, Y. P. Siwakoti, S. A. Gorji *et al*., "A survey on voltage boosting techniques for step-up DC-DC converters," in *Proceedings of IEEE Energy Conversion Congress and Exposition (ECCE)*, Milwaukee, USA, Sept. 2016, pp. 1-8.

[26] R. Kahani, M. Jamil, and M. T. Iqbal, "Direct model reference adaptive control of a boost converter for voltage regulation in microgrids," *Energies*, vol. 15, no. 14, p. 5080, Jul. 2022.

[27] E. Mamarelis, G. Petrone, and G. Spagnuolo, "Design of a sliding modecontrolled SEPIC for PV MPPT applications," *IEEE Transactions on Industrial Electronics*, vol. 61, no. 7, pp. 3387-3398, Jul. 2014.

[28] S. J. Chiang and H. J. Shieh, "Modeling and control of PV charger system with SEPIC converter," *IEEE Transactions on Industrial Electronics*, vol. 56, no. 11, pp. 4344-4353, Nov. 2009.

[29] R. F. Rajakumari and M. Deshpande, "Comparative analysis of DC-DC converters," in *Proceedings of 2nd International Conference on Power and Embedded Drive Control (ICPEDC)*, Chennai, India, Aug. 2019, pp. 504-509.

[30] J. Thongprona, K. Kirtikara, and C. Jivacate, "A method for the determination of dynamic resistance of photovoltaic modules under illumination," *Solar Energy Materials and Solar Cells*, vol. 90, no. 18, pp. 3078-3084, Nov. 2006.

[31] A. Mäki, S. Valkealahti, and T. Suntio, "Dynamic terminal characteristics of a photovoltaic generator," in *Proceedings of 14th International Power Electronics and Motion Control Conference*, Skopie, Republic of Macedonia, Sept. 2010, pp. 12-76.

[32] A. Urtasun, P. Sanchis, and L. Marroyo, "Adaptive voltage control of the DC/DC boost stage in PV converters with small input capacitor," *IEEE Transactions on Power Electronics*, vol. 28, no. 11, pp. 5038-5048, Nov. 2013.

[33] R. Lin, Y. Chang, and C. Lee, "Optimal design of LED array for single-loop CCM buck-boost LED driver," *IEEE Transactions on Industrial Application*, vol. 49, no. 2, pp. 761-768, Mar. 2013.

[34] E. P. Sarika, J. Jacob, S. S. Mohammed *et al*., "Standalone PV system with modified VSS P&O MPPT controller suitable for partial shading conditions," in *Proceedings of 2021 7th International Conference on Electrical Energy Systems (ICEES)*, Tamil Nadu, India, Feb. 2021, pp. 51-55.

Rasool Kahani received the B.Sc. degree of electronic engineering from Islamic Azad University, Tehran, Iran, in 2008, and the M.Sc. degree of control engineering from Islamic Azad University, in 2012. He is also pursuing the M.Eng. in electrical engineering in Memorial University of Newfoundland, St. John's, Canada. His research interests include control system theory, renewable energy systems, power electronic converters, and smart grids.

Mohsin Jamil received the B.Eng. degree in industrial electronics from Nadir Edulgee Dinshaw (NED) University, Karachi, Pakistan, in 2004, the master's degree from Dalarna University, Falun, Sweden, in 2006, the master's degree from the National University of Singapore, Singapore, in 2008, and the Ph.D. degree from the University of Southampton, Southampton, UK, in 2012. His research interests include renewable energy systems, hybrid power systems, power electronic converters, and smart grids.

M. Tariq Iqbal received the B.Sc. (EE) degree from the University of Engineering and Technology, Lahore, Pakistan, in 1986, the M.Sc. degree in nuclear engineering from the Quaid-e-Azam University, Islamabad, Pakistan, in 1988, and the Ph.D. degree in electrical engineering from the Imperial College London, London, UK, in 1994. His research interests include hybrid power systems, renewable energy systems, passive houses and electronics and control systems.